Published OnlineFirst October 1, 2014; DOI: 10.1158/0008-5472.CAN-14-1482

Cancer Research

Tumor-Derived Osteopontin Suppresses Antitumor Immunity by Promoting Extramedullary Myelopoiesis

Eun-Kyung Kim[1], Insu Jeon[2], Hyungseok Seo[2], Young-Jun Park[1], Boyeong Song[2], Kyoo-A Lee[1], Yongwoo Jang[2], Yeonseok Chung[1], and Chang-Yuil Kang[1,2]

Abstract

Extramedullary myelopoiesis occurs commonly in tumor-bearing animals and is known to lead to accumulation of peripheral myeloid-derived suppressor cells (MDSC), which play an important role in immune escape. However, the cellular and molecular mechanisms by which tumors induce extramedullary myelopoiesis are poorly understood. In this study, we found that osteopontin expressed by tumor cells enhances extramedullary myelopoiesis in a CD44-dependent manner through the Erk1/2–MAPK pathway. Osteopontin-mediated extramedullary myelopoiesis was directly associated with increased MDSCs in tumor-bearing hosts. More importantly, osteopontin silencing in tumor cells delayed both tumor growth and extramedullary myelopoiesis, while the same treatment did not affect tumor growth *in vitro*. Finally, treatment with an antibody against osteopontin inhibited tumor growth and synergized with cell-based immunotherapeutic vaccines in mediating antitumor immunity. Our findings unveil a novel immunosuppressive role for tumor-derived osteopontin and offer a rationale for its therapeutic targeting in cancer treatment. *Cancer Res; 74(22); 1–12. ©2014 AACR.*

Introduction

Tumors can escape host immune surveillance by recruiting various tumor-associated myeloid cells that create an immunosuppressive environment in tumor-bearing hosts (1). Recent studies have identified the ontogeny and phenotype of such tumor-associated myeloid cells. Stemming from bone marrow hematopoietic stem cells, common myeloid progenitors consist of heterogeneous myeloid cell populations such as tumor-associated macrophages, tumor-associated neutrophils, $Tie2^+$ monocytes, and myeloid-derived suppressor cells (MDSC; refs. 2, 3). Among them, MDSCs, which are a heterogeneous population of monocytic and granulocytic immature cells (4), are well characterized as playing a pivotal role in establishing an immunosuppressive network and eventually incapacitating multiple arms of antitumor immunity (5–12). MDSCs can be induced by diverse inflammatory conditions such as tumor, infection, and injury. Importantly, the frequency of peripheral MDSCs clinically correlates with poor prognosis in patients with cancer (9, 13–15), indicating a detrimental role of this cellular subset in the host defense against cancer.

Immune cells originate from the pluripotent hematopoietic stem cell ($lineage^{neg}/CD127^-/CD117^+/Sca1^+$, LSK cells). LSK cells can be further differentiated into $lineage^{neg}/CD127^-/CD117^+/Sca1^-$ myeloid progenitor populations (LK cells) and $lineage^{neg}/CD127^+/CD117^+/Sca1^+$ common lymphoid progenitors. Chronic inflammatory environments that include tumor-bearing conditions are known to trigger dysregulated hematopoiesis, leading to excessive myelopoiesis and increased MDSCs (7, 9, 16). In particular, tumor growth can induce myelopoiesis outside the bone marrow, including the spleen (17–20), which is termed extramedullary myelopoiesis. Extramedullary myelopoiesis is thought to cause tumor-associated myeloid cell accumulation in the spleens of tumor-bearing hosts (20).

Although tumor-induced inflammation is thought to trigger extramedullary myelopoiesis, the identity and origin of the factors that mediate this phenomenon as well as the molecular mechanism by which those factors trigger extramedullary myelopoiesis remain poorly understood. In this study, we observed increased levels of osteopontin in tumor-bearing mice (TBM), and this osteopontin was mainly derived from tumor cells. Moreover, tumor-derived osteopontin was found to enhance extramedullary myelopoiesis and the subsequent accumulation of MDSCs in the spleens of TBM. Furthermore, the administration of an antiosteopontin antibody in TBM significantly improved the anticancer effect of the cell-based immunotherapeutic vaccine.

[1]Laboratory of Immunology, Research Institute of Pharmaceutical Sciences, College of Pharmacy, Seoul National University, Gwanak-gu, Seoul, Korea. [2]Department of Molecular Medicine and Biopharmaceutical Sciences, Graduate School of Convergence Science and Technology, and College of Medicine or College of Pharmacy, Seoul National University, Gwanak-gu, Seoul, Korea.

Note: Supplementary data for this article are available at Cancer Research Online (http://cancerres.aacrjournals.org/).

Current address for Y. Jang: McLean Hospital, Harvard Medical School, Belmont, MA 02478; and current address for K.-A. Lee, Department of Immunology, College of Medicine, Mayo Clinic, Rochester, MN.

Corresponding Author: Chang-Yuil Kang, Laboratory of Immunology, College of Pharmacy, Seoul National University, Sillim-dong, Gwanak-gu, Seoul 151742, Korea. Phone: 822-880-7860; Fax: 822-885-1373; E-mail: cykang@snu.ac.kr

doi: 10.1158/0008-5472.CAN-14-1482

Published OnlineFirst October 1, 2014; DOI: 10.1158/0008-5472.CAN-14-1482

Materials and Methods

Mice and tumor model

Balb/c mice and C57BL/6 were purchased from the Charles River Laboratories. All mice were maintained in specific pathogen—free conditions, and the Institutional Animal Care and Use Committee of Seoul National University approved all of the animal experiments conducted in this study. For the murine tumor model studies, 3×10^5 of the indicated tumor cells were injected subcutaneously into the left flake of naïve mice. TBM were used for experiments 3 to 4 weeks after tumor injection.

Antibodies for flow cytometry analysis and ELISA

The antibodies for flow cytometry were purchased from either Biolegend or eBioscience. To detect hematopoietic stem cells and myeloid progenitor cells, FITC-conjugated lineage markers (CD3ε, B220, CD11b, Gr1, TER-119), FITC or APC-cy7–conjugated CD127 (A7R34), phycoerythrin (PE) or APC-conjugated CD16/32 (93), PE-cy7–conjugated CD117 (2B8), PE-cy5–conjugated Sca-1 (D7), and APC or eFluor 450–conjugated CD34 (RAM34) were used. To analyze the surface molecules on LK cells, APC-conjugated CD29 (HMβ1-1), CD44 (IM7), CD61 (HMβ3-1), PE-conjugated CD49d (R1-2), and CD51 (RMV7) were used. To detect MDSCs and T cells, FITC-conjugated Ly6C (HK1.4), PE-cy7–conjugated Ly6G (1A8), APC-conjugated CD11b (M1/70), PerCP-cy5.5–conjugated CD4 (GK1.5), APC-cy7–conjugated CD8α (53-6.7), PE or eFluor 450–conjugated CD3ε (145-2C11) were used. The flow cytometric analysis was performed using FACSAriaIII (BD Biosciences). For the ELISA and Western blot analyses, goat–anti-mouse osteopontin (Sigma, Sigma Aldrich), recombinant mouse osteopontin (rmOpn) and biotinylated goat-anti-mouse osteopontin (R&D Systems) were used.

Cell culture

MPIIB10 hybridoma was purchased from Developmental Studies Hybridoma Bank and cultured in RPMI medium (GIBCO) that was supplemented with 10% FBS (GIBCO) and 1% penicillin/streptomycin (Lonza) and 500μg/mL of Geneticin (GIBCO). The CT26 and MC38 colon carcinoma cells were cultured in DMEM medium that was supplemented with 10% FBS and 1% penicillin/streptomycin.

Mouse osteopontin lentiviral vector and shRNA transfection

The GIPZ lentiviral shRNA vector for mouse osteopontin knockdown (RMM4532-NM_009263, pGIPZ-shOpn) and GIPZ nonsilencing lentiviral shRNA control (RHS4346, pGIPZ) were purchased from Open Biosystems. The Trans-lentiviral shRNA packaging kit was used for lentiviral particle production according to the manufacturer's instructions (Open Biosystems). To establish CT26 osteopontin knockdown or control cells, pGIPZ-shOpn or control pGIPZ–containing lentiviral particles were transfected into CT26 cells according to the manufacturer's instructions. The transfected CT26 cells were selected and subcloned in 10 μg/mL puromycin-containing medium.

Evaluation of *in vitro* proliferation of the tumor cells

First, 2×10^4 of CT26shopn or CT26pGIPZ cells were cultured on 8-well chamber slide plates. After 2 days of culture, cells were harvested, fixed with 70% ethanol, and then stained intracellularly with an Alexa 647–conjugated Ki67 antibody (M-19, Santa Cruz Biotechnology). To analyze cell numbers, the cells were fixed with 4% paraformaldehyde and then stained with Hoechst 33342, a nucleus marker (Invitrogen, KDR Biotech). The fluorescent images were acquired at 350 nm excitation using a fluorescence microscope, and the cell numbers were counted using the ImageJ software.

For a quantitative analysis of cell proliferation, 2×10^4 of CT26shopn or CT26pGIPZ cells were cultured on 96-well plate in the presence of 1 μCi/well [^{3}H]-thymidine (Perkin Elmer) for 48 hours, and the [^{3}H]-thymidine incorporation was detected by Liquid Scintillation Counter (Tri-Carb LSC, Perkin Elmer).

Cytokine array

For the comparative analysis of the levels of various cytokines and chemokines in spleen lysates, cytokine array kits (R&D Systems, ARY-015 and ARY-006) were used according to the manufacturer's protocol. The mean spot density was measured using the ImageJ software (Free software distributed by NIH, Bethesda, MD), and mean values above the reference (mean spot density of negative control spot) were charted on a graph using the GraphPad Prism software.

Quantitative real-time PCR

The RNeasy Mini Kit (Qiagen), amfiRivert Platinum (GenDEPOT), SYBR Premix ExTaq (Takara), and the LightCycler optical system (Roche) were used for quantitative real-time PCR. The following primers were used: murine *Hprt* forward (AAG ACT TGC TCG AGA TGT CAT GAA), and murine *Hprt* reverse (ATC CAG CAG GTC AGC AAA GAA), murine *Spp1* forward (CCG AGG TGA TAG CTT GGnC TT), murine *Spp1* reverse (CTG CCC TTT CCG TTG TTG TC).

Bromodeoxyuridine incorporation

For *in vivo* bromodeoxyuridine (BrdUrd) incorporation analysis, 500 mg/kg of BrdUrd was injected intraperitoneally into naïve Balb/c mice and mice bearing CT26pGIPZ or CT26shOpn tumor cells. Mice were sacrificed 26 days after tumor injection. Splenocytes and bone marrow cells were surface stained and then incorporated. BrdUrd was intracellularly stained using the APC BrdUrd Flow Kit (BD Pharmigen). For *in vitro* BrdUrd incorporation analysis, total splenocytes from 3-week CT26 TBM were cultured in STEMPRO34 serum-free medium (GIBCO) supplemented with 1% penicillin/streptomycin, 2 mmol/L L-glutamic acid, nutrient supplement (40× stock supplemented with STEMPRO34), 10 ng/mL rmIL3, 10 ng/mL rmIL6, and 10 ng/mL rmSCF (STEMPRO34 complete medium) with or without 2 μg/mL osteopontin. In some experiments, 20 μg/mL of the indicated blocking antibodies or 20 μmol/L of PD98059 (Sigma Aldrich) was also added to the culture media. After 24 hours of culture, BrdUrd was added at a final concentration of 1 μg/mL and incubated for an additional 24 hours. BrdUrd incorporation was measured as described above.

Published OnlineFirst October 1, 2014; DOI: 10.1158/0008-5472.CAN-14-1482

In vivo treatment of osteopontin

Here, 4 μg of recombinant mouse osteopontin (R&D Systems, reconstituted in PBS) or PBS was intravenously injected in naïve Balb/c mice at day 0, 2, 4, and 6. The mice were sacrificed at day 7 and hematopoietic progenitor cells in the spleen were analyzed by flow cytometric analysis.

Western blotting

For the Western blot assays, the following antibodies were used: α-rabbit-phospho Erk1/2$^{(Thr202/204)}$, α-rabbit-Erk1/2, α-rabbit-cyclinD1, α-rabbit-phospho Rb$^{(Ser807/811)}$ (D20B12) α-rabbit-Rb (D20; Cell Signaling Technology). LK cells from 3-week CT26 TBM were isolated using a FACSAriaIII, and 1×10^5 of the isolated cells were rested for 1 hour. Then, the cells were stimulated with 2 μg/mL of rm-osteopontin for 5 minutes. After stimulation, the cells were harvested and processed for Western blot assays.

Therapeutic tumor model

The mice were subcutaneously injected with CT26 or MC38 tumors (3×10^5 cells) on day 0. Seven days after tumor injection, mice were intraperitoneally injected with 0.5 mg of antiosteopontin (MPIIIB10) or mIgG as control every other day for 10 days. Some mice were also given a B-cell–based vaccine on day 9 (MC38 model) or day 10 (CT26 model). The B-cell–based therapeutic vaccines were prepared as described previously (21) using the H-2^d epitope peptide of gp70 of CT26 tumor (AH1 6-14, SPSYVYHQF) or the H-2^d epitope peptide of gp70 of MC38 tumor (p15E 604-611, KSPWFTTL; ref. 22).

Statistical analysis

The data are shown as the mean ± SEM. Statistical significance was analyzed by GraphPad Prism software. A two-tailed Student *t* test or two-way ANOVA was used to calculate statistical significance and *P* values <0.05 were considered significant at a 95% confidence interval.

Results

Tumor growth enhances extramedullary myelopoiesis and subsequent accumulation of MDSCs.

MDSCs rapidly accumulate in the spleen and at the tumor site in tumor-bearing hosts, concomitant with tumor growth. When Balb/c mice were inoculated with CT26 tumor cells, the number of total splenocytes increased by 2-fold 21 days after tumor injection (Supplementary Fig. S2A). The percentages and number of both monocytic (Mo) MDSCs (CD11b$^+$/Ly6C^{hi}/Ly6G^{lo}) and polymorphonuclear (PMN) MDSCs (CD11b$^+$/Ly6C^{lo}/Ly6G^{hi}) were greatly increased in the spleens of TBM (Supplementary Fig. S2B). In contrast, the percentages of CD4$^+$ and CD8$^+$ T lymphocytes were decreased, whereas the absolute number of T lymphocytes remained unchanged (Supplementary Fig. S2C).

Because chronic inflammation, including tumor-bearing condition, induces hematopoietic proliferation and differentiation in the spleen as well as in the bone marrow (17–20), we next examined whether the observed accumulation of MDSCs in TBM was caused by hematopoietic dysregulation, especially extramedullary myelopoiesis. To this end, we analyzed the frequencies and absolute numbers of diverse hematopoietic cell populations including hematopoietic stem cells (Lineage^{neg}/CD127$^-$/CD117$^+$/Sca1$^+$, LSK cells), heterogeneous myeloid progenitors (Lineage^{neg}/CD127$^-$/CD117$^+$/Sca1$^-$, LK cells), and common lymphoid progenitors (lineage^{neg}/CD127$^+$/CD117^{int}/Sca1^{low}). Notably, we observed that the frequencies and numbers of LK cells and LSK cells were significantly increased in the splenocytes of TBM (Fig. 1A), whereas the frequencies of common lymphoid progenitors remained comparable with those of naïve mice (Supplementary Fig. S2D). We observed a similar increase in the MDSC, LK, and LSK populations in the spleen when MC38 tumor cells were used (Fig. 1B and Supplementary Fig. S3).

To further address whether the abnormal accumulation of MDSCs is due to increased LK and LSK populations in the spleens of tumor-bearing hosts, we transferred a mixture of LSK and LK cells isolated from the spleen of MC38 tumor-bearing congenic C57BL/6 mice (CD45.1$^{+/+}$) into MC38 tumor-bearing C57BL/6 mice (CD45.2$^{+/+}$). We observed that more than 80% of the donor cells were converted into CD11b$^+$ myeloid cells, primarily PMN MDSCs, and Mo MDSCs (Fig. 1C and D). Similar results were obtained when a mixture of LSK and LK donor cells (CD45.2$^+$) were transferred into a CD45.1$^+$ MC38 tumor-bearing recipients (Supplementary Fig. S2E). Taken together, these results indicate that increased peripheral LK cells and LSK cells in the tumor context induced extramedullary myelopoiesis, which was consequently responsible for MDSC expansion.

Osteopontin is increased in TBM

Given that the accumulation of LK and LSK cells was observed in the spleens, we hypothesized that soluble factor(s) derived from or induced by tumor cells are responsible for the increased myelopoiesis in the spleens. Therefore, we comparatively analyzed the levels of various cytokines and chemokines in the spleen lysates of naïve and TBM with cytokine arrays. As depicted in Fig. 2A and B, we observed that the levels of CD26, CXCL1, CCL2, and osteopontin were higher in the spleen of TBM compared with naïve mice. Among these factors, osteopontin has been shown to promote the growth and progression of certain solid tumors (23–28), and is known as a key component of the hematopoietic niche in bone marrow (29, 30). However, the role of osteopontin in extramedullary myelopoiesis remains poorly understood. Thus, we sought to address the role of osteopontin in the observed increased extramedullary myelopoiesis in the tumor context. To confirm the cytokine array data, we analyzed the amount of osteopontin in spleen lysates and sera by ELISA and found that osteopontin was consistently increased in the spleen and sera of CT26 TBM (Fig. 2C). Using real-time PCR analysis, we found that increased osteopontin was mainly produced by tumor tissue (Fig. 2E) rather than Mo MDSC (Fig. 2D). Increased levels of osteopontin were also observed when MC38 tumor cells were used in a similar experimental setting (Supplementary Fig. S4A and S4B).

Published OnlineFirst October 1, 2014; DOI: 10.1158/0008-5472.CAN-14-1482

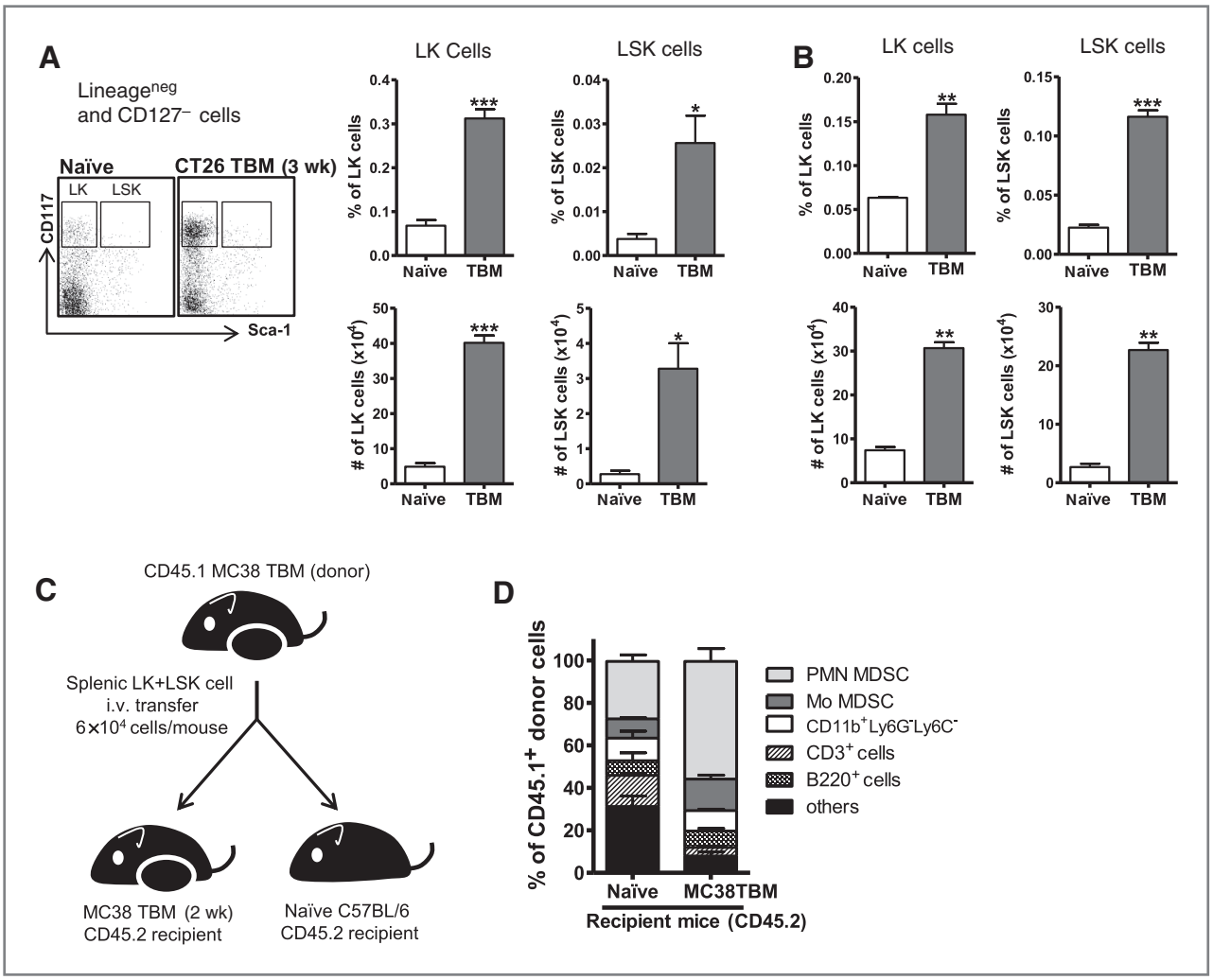

Figure 1. Accumulated hematopoietic progenitor cells and enhanced extramedullary myelopoiesis in the tumor environment Balb/c mice were subcutaneously injected with CT26 cells (3×10^5cells). A, the absolute numbers and frequencies of LK and LSK cells in the splenocytes of naïve mice or CT26 TBM. B, the absolute numbers and frequencies of LK and LSK cells in the splenocytes of naïve mice or MC38 TBM. The data are representative of three independent experiments and represent the mean ± SEM ($n = 3$; *, $P < 0.05$; **, $P < 0.01$; ***, $P < 0.001$). C, LK cells and LSK cells were sorted from MC38 tumor bearing CD45.1$^{+/+}$ congenic C57BL/6 mice and intravenously transferred to naïve or MC38 tumor bearing (2-week) CD45.2$^{+/+}$ C57BL/6 mice. D, seven days after donor cell transfer, CD45.1$^{+/+}$ donor cells in the spleen were analyzed.

Tumor-derived osteopontin facilitates *in vivo* tumor growth and subsequent increase of splenic LK cells

To directly address the role of tumor-derived osteopontin, we established a CT26 tumor cell line in which osteopontin was knocked down by transfecting an osteopontin-specific shRNA containing lentiviral vector (CT26shOpn). CT26 cells transfected with empty lentiviral vector were used as control (CT26pGIPZ). The knock down of osteopontin in the CT26shOpn was confirmed by Western blot analysis (Fig. 3A). As shown in Fig. 3B and C, the knockdown of osteopontin did not affect the proliferation of CT26 tumor cells *in vitro*.

We next subcutaneously inoculated CT26pGIPZ and CT26shOpn tumor cells in naïve Balb/c mice and monitored tumor growth. In contrast to tumor growth *in vitro* (Fig. 3B and C), the growth of CT26shOpn cells in mice was significantly delayed compared with that of cells expressing CT26pGIPZ (Fig. 3D). Therefore, we sought to determine whether the observed difference in the tumor growth *in vivo* was due to decreased proliferation or increased apoptosis of the CT26shOpn tumor cells by using Ki67 or Annexin V immunostaining, respectively. The *in vivo* proliferation of CT26shOpn was found to be comparable with that of CT26pGIPZ (Supplementary Fig. S5A). In contrast, the apoptosis of CT26shOpn cells was remarkably higher than that of CT26pGIPZ cells (Supplementary Fig. S5B). In addition, the cellularity in the spleens of CT26shOpn-injected mice was far less than that of CT26pGIPZ-injected mice. As expected, the levels of osteopontin in the sera and tumor tissues were lower in the CT26shOpn-injected mice than those in the CT26pGIPZ group (Fig. 3E). Taken together, these results indicate that tumor-derived osteopontin contributes to tumor growth, presumably through the suppression of tumor cell apoptosis induced by

Published OnlineFirst October 1, 2014; DOI: 10.1158/0008-5472.CAN-14-1482

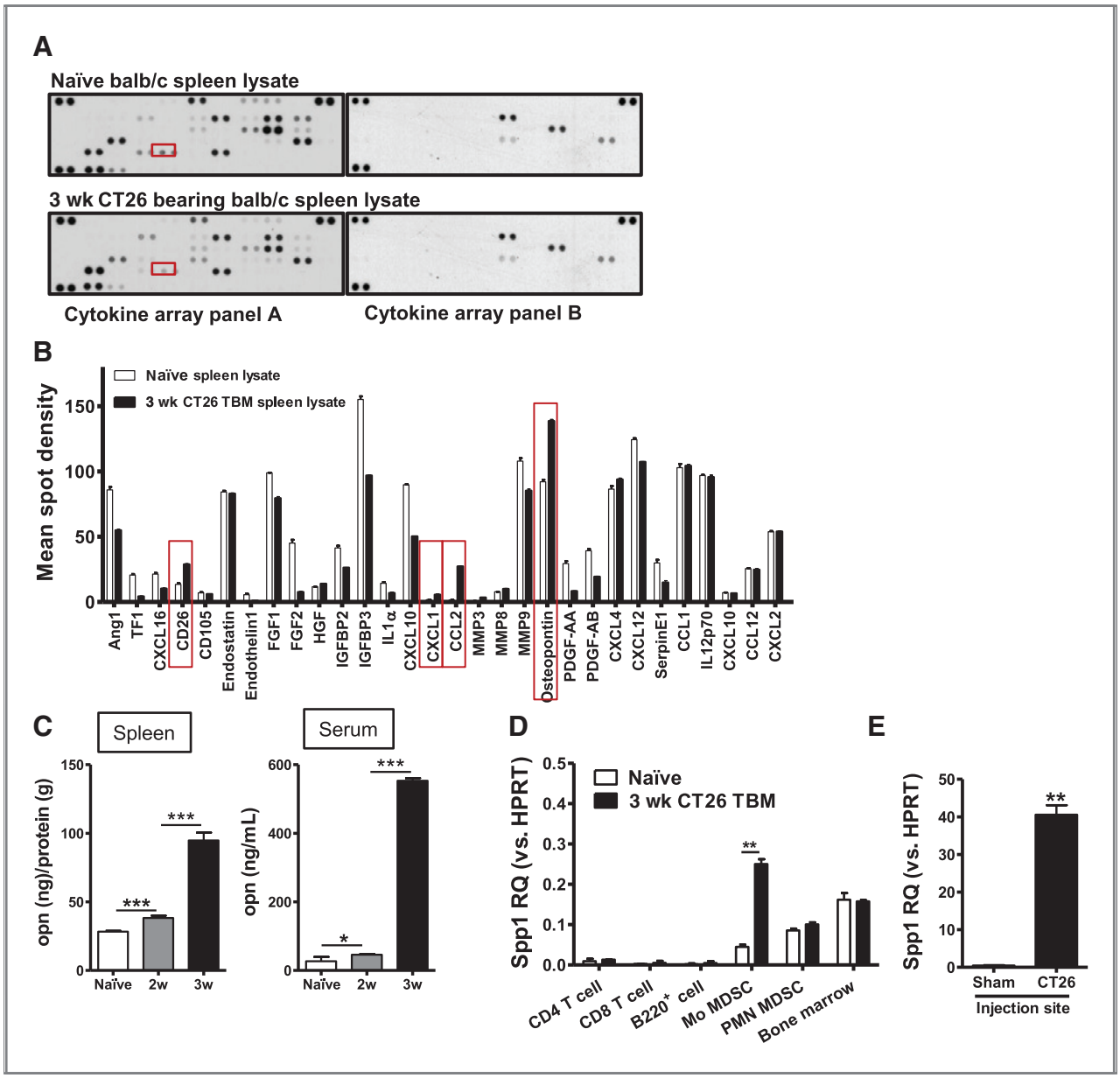

Figure 2. Osteopontin increased in the tumor environment. A, comparative cytokine levels in the spleen lysates of naïve Balb/c mouse and 3-week CT26 TBM were measured. B, the mean densities of each spot were measured and mean values above reference were charted on the graph. The data are representative of three independent experiments. C, the concentrations of osteopontin in spleen lysate and serum. D, the *Spp1* (osteopontin) mRNA levels in $CD4^+$ T cell, $CD8^+$ T cell, B-cell, Mo MDSC, PMN MDSC, and total bone marrow cells. E, the *Spp1* mRNA levels in injection site. All data are representative of three independent experiments and represent the mean ± SEM ($n = 3$; *, $P < 0.05$; **, $P < 0.01$; ***, $P < 0.001$).

immune cells or a mechanism other than an autocrine effect on tumor cells.

To further investigate the possible role of tumor site–derived osteopontin in extramedullary myelopoiesis, we analyzed hematopoietic progenitor cell populations in the splenocytes of the naïve, CT26pGIPZ-bearing, or CT26shOpn-bearing mice. As expected, the frequencies and absolute numbers of LK and LSK population were increased in the CT26pGIPZ and CT26shOpn groups compared with naïve mice. Importantly, however, the extent of the increase of the LK cell population was significantly lower in the CT26shOpn group than CT26pGIPZ group, whereas the LSK cell population remained comparable between the two groups (Fig. 3F). The LK cells represent heterogenous myeloid progenitor populations that include common myeloid progenitors (CMP, $LK/CD34^+/Fc\gamma R^{low}$), granulocyte-macrophage progenitors (GMP, $LK/CD34^+/Fc\gamma R^{high}$), and megakaryocyte-erythroid progenitors (MEP, $LK/CD34^-/Fc\gamma R^-$). The CMP, GMP, and MEP populations were all similarly, but profoundly, decreased in the CT26shOpn group in comparison with the

Published OnlineFirst October 1, 2014; DOI: 10.1158/0008-5472.CAN-14-1482

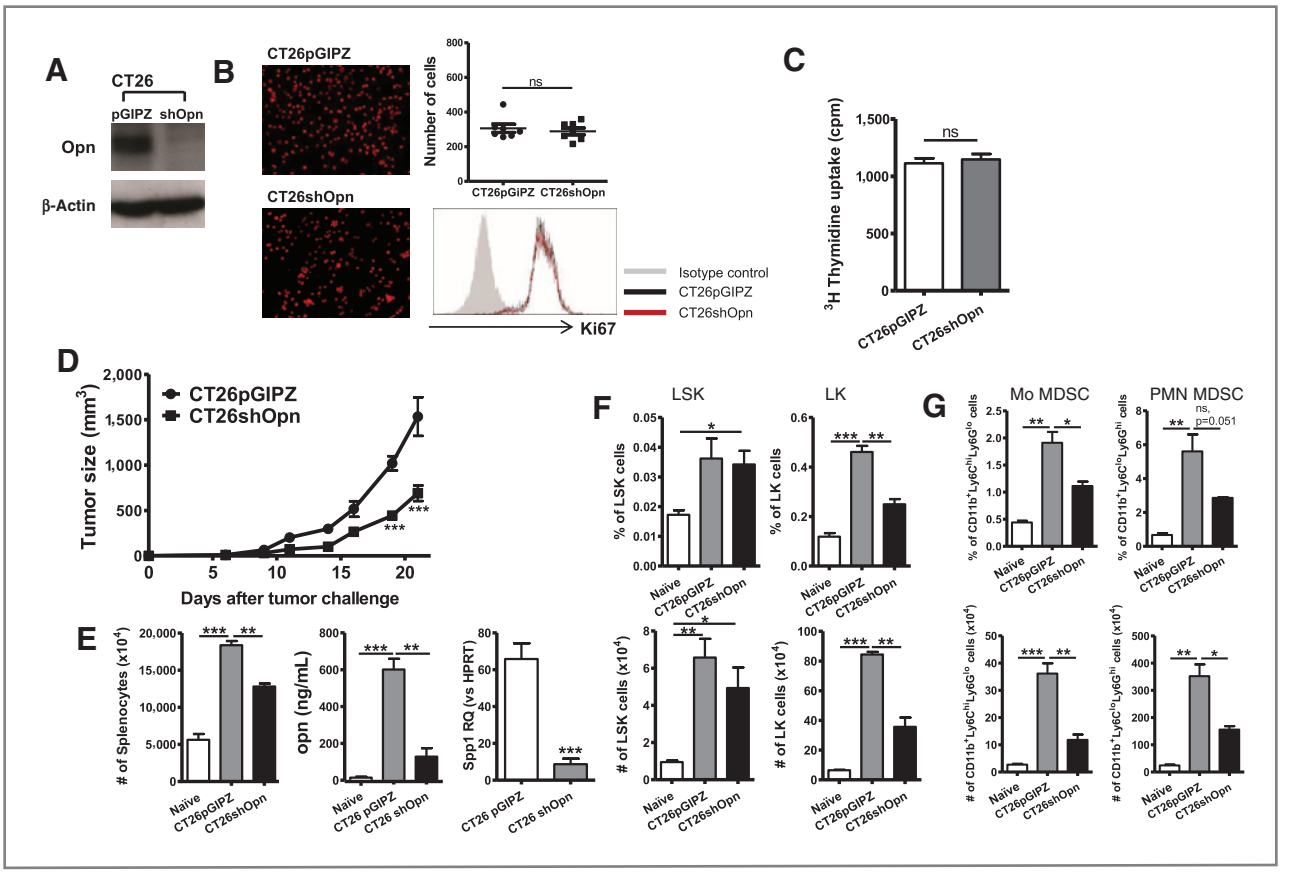

Figure 3. Construction of an osteopontin knockdown CT26 tumor cell line and the effect on *in vivo* tumor growth and subsequent increase of splenic LK cells A, osteopontin protein levels in the CT26pGIPZ or CT26shOpn were analyzed by Western blotting. B, *in vitro* proliferation of CT26pGIPZ or CT26shOpn. C, incorporated [^{3}H]Thymidine of CT26pGIPZ or CT26shOpn. D, Balb/c mice were subcutaneously injected with 3×10^5 cells of CT26pGIPZ or CT26shOpn cells. Six days after tumor injection, tumor size was measured every 2 or 3 days ($n = 5$). E, the numbers of total splenocytes at 21 days after tumor injection (left). The concentration of osteopontin in the serum (middle). *Spp1* mRNA expression in the tumor tissues (right). F, the percentages and numbers of LSK cells, LK cells. G. the percentages and numbers of Mo MDSCs and PMN MDSCs. All data are representative of three independent experiments and represent the mean ± SEM (*, $P < 0.05$; **, $P < 0.01$; ***, $P < 0.001$). ns, nonsignificant.

CT26pGIPZ group (Supplementary Fig. S6). Furthermore, the frequencies and absolute numbers of Mo MDSCs and PMN MDSCs were also significantly lower in the CT26shOpn group than in the CT26pGIPZ group, although they were still higher than those of the naïve group (Fig. 3G). These results demonstrate that tumor site–derived osteopontin facilitates tumor growth *in vivo*, presumably by leading to the increase of splenic LK cells and subsequent MDSC accumulation.

We next addressed whether the reduced accumulation of MDSCs in the CT26shOpn-TBM was due to the difference in the size of tumor mass. We established mice bearing CT26pGIPZ or CT26shOpn tumors with similar tumor masses at day 10 by injecting 3.3 times higher number of the latter tumor cells into naïve mice (Supplementary Fig. S7A). In this experimental setting, we observed that the serum levels of osteopontin as well as the frequencies of splenic LK cells and Mo MDSCs cells were significantly reduced in the CT26shOpn-bearing mice compared with the CT26pGIPZ-bearing mice (Supplementary Fig. S7B, S7D, and S7E). The elevated osteopontin in the CT26pGIPZ TBM was found to be mainly from the inoculated malignant cells (Supplementary Fig. S7C). These results collectively demonstrated that the elevated level of osteopontin in TBM was responsible for the extramedullary myelopoiesis during the early stage of tumor progression, independently of tumor mass.

Tumor-derived osteopontin increases proliferation of myeloid progenitor (LK) cells

We next sought to determine the mechanism by which tumor-derived osteopontin increases splenic LK cells. We first determined whether osteopontin directly induces the proliferation of LK cells in TBM. Mice bearing CT26pGIPZ or CT26shOpn were injected with BrdUrd before the analysis of BrdUrd incorporation in splenocytes (Fig. 4A). Again, tumor growth was remarkably delayed in the CT26shOpn-injected mice compared with CT26pGIPZ-injected mice (Fig. 4B). The BrdUrd incorporation of bone marrow LK cells was comparable among the naïve, CT26pGIPZ, and CT26shOpn groups. In sharp contrast, BrdUrd incorporation was significantly increased in the splenic LK cells

Published OnlineFirst October 1, 2014; DOI: 10.1158/0008-5472.CAN-14-1482

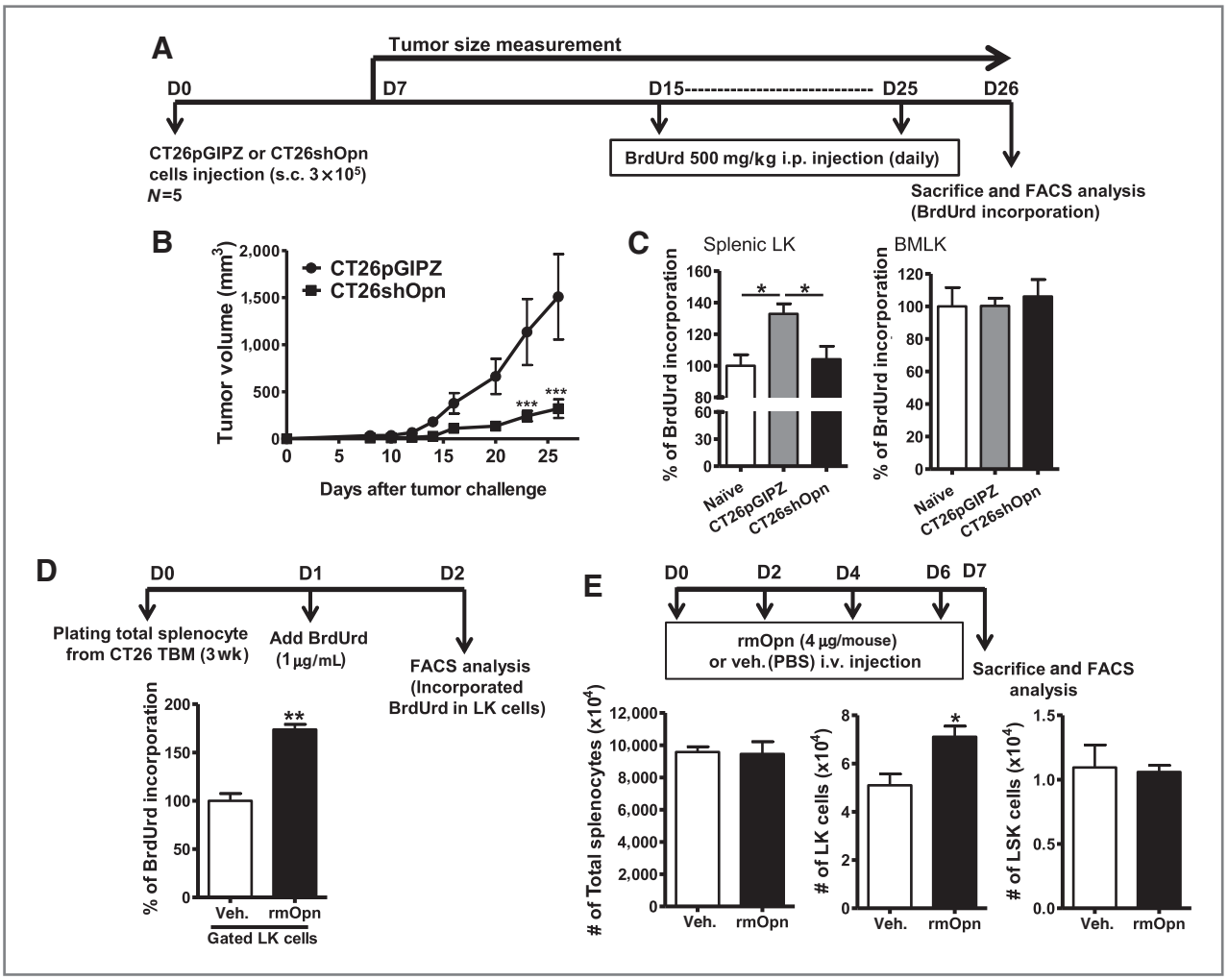

Figure 4. Expansion of splenic LK cells by tumor-derived osteopontin. A, Balb/c mice were subcutaneously injected with CT26pGIPZ or CT26shOpn cells and 500 mg/kg BrdUrd was daily injected from 15 to 25 days after tumor injection. B, seven days after tumor injection, tumor size was measured every 2 or 3 days ($n = 5$). C, the incorporation of BrdUrd in spleen and bone marrow LK cells was analyzed by flow cytometry. D, the experimental scheme for *in vitro* BrdUrd incorporation (top) and incorporated BrdUrd in the splenic LK cells (bottom). All data are representative of two independent experiments and represent the mean ± SEM (*, $P < 0.05$; **, $P < 0.01$; ***, $P < 0.001$). E, Balb/c mice were intravenously injected with 4 μg of rmOpn (dissolved in PBS) or vehicle at day 0, 2, 4, and 6. At day 7, mice were sacrificed and the LK and LSK cells in the spleen were analyzed.

of the CT26pGIPZ group compared with naïve mice (Fig. 4C). To determine whether osteopontin directly stimulates the expansion of LK cells, we cultured splenocytes in the presence of recombinant osteopontin and found that this cytokine induced the proliferation of the LK population *in vitro* (Fig. 4D). Consistently, the injection of recombinant osteopontin slightly but significantly increased the number of LK cells in the spleen of naïve Balb/c mice, whereas the number of LSK cells remained unchanged (Fig. 4E).

To determine whether osteopontin induced the migration of LK cells, we performed Transwell chemotaxis assay and found that osteopontin weakly induced the migration of LK cells (Supplementary Fig. S8A). However, osteopontin did not affect the migration (data not shown) or survival of MDSCs *in vitro* (Supplementary Fig. S8B). Collectively, these results demonstrate that osteopontin primarily affected LK cells rather than MDSCs.

CD44 is a main receptor that mediates osteopontin-induced proliferation of LK cells

To further investigate the mechanism of osteopontin-mediated proliferation of the LK population, we examined the expression of known osteopontin receptors on LK cells. Among the known osteopontin receptors, the levels of CD44 and CD49d (integrin α4) expression were significantly increased in the splenic LK cells of the CT26pGIPZ group compared with those of LK cells in naïve mice, whereas those of CD51 (integrin αv) and CD61 (integrin β3) were reduced in the splenic LK cells of CT26pGIPZ-injected mice (Fig. 5A). Interestingly, the levels of CD44, CD49d, and CD29 (integrin β1) were significantly lower in the LK cells

Published OnlineFirst October 1, 2014; DOI: 10.1158/0008-5472.CAN-14-1482

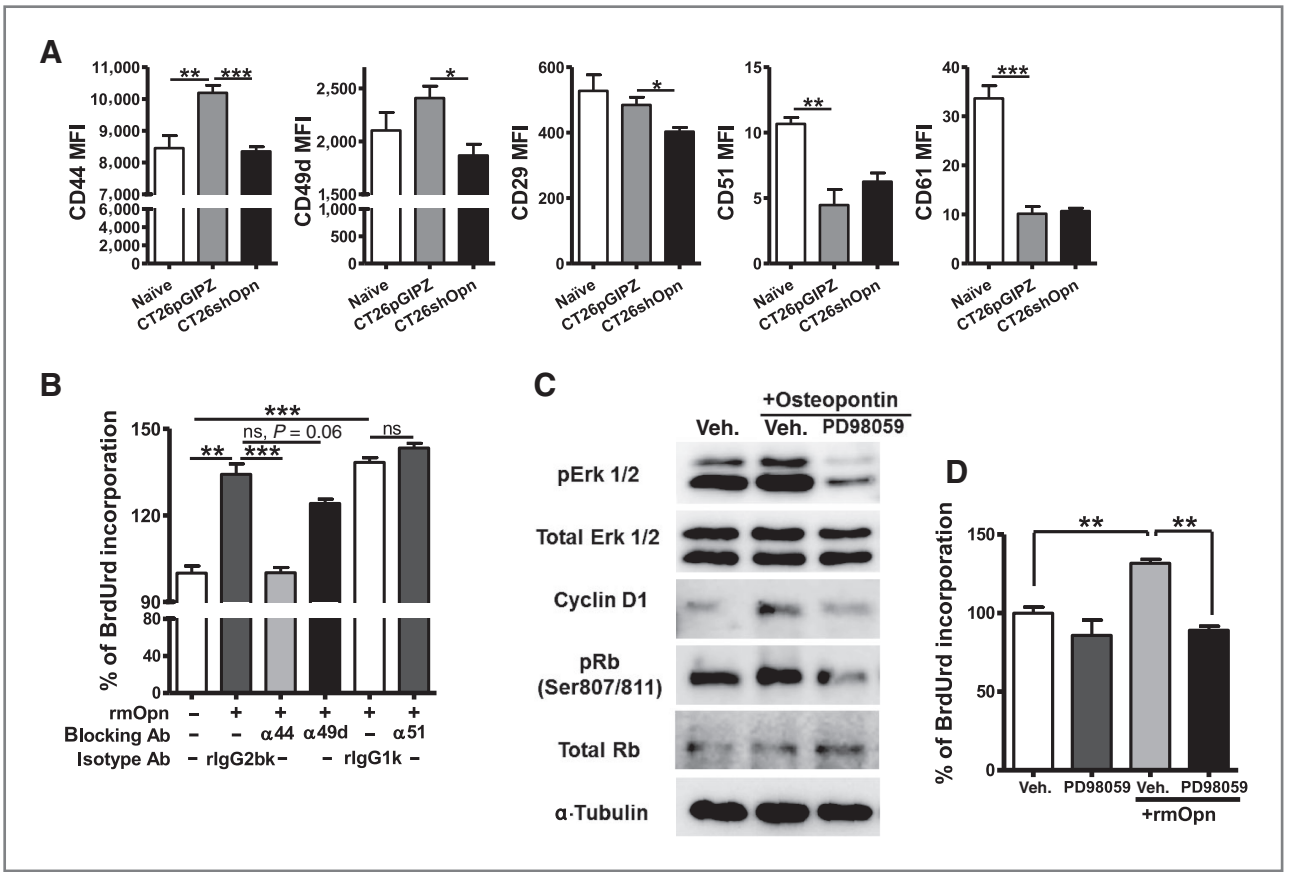

Figure 5. Mechanisms of osteopontin-induced proliferation of LK cells. A, the expression levels of CD44, CD49d, CD29, CD51, and CD61 on the splenic LK cells of naïve mice and mice bearing CT26pGIPZ or CT26shOpn ($n = 3$). The mean fluorescence intensity (MFI) values were normalized to the MFI values of an isotype control antibody. B, the incorporation of BrdUrd in LK cells of *in vitro* cultured total splenocytes from CT26 TBM with or without 20 μg/mL indicated blocking antibody and 2 μg/mL rmOpn. The data are representative of two independent experiments and represent the mean ± SEM (*, $P < 0.05$; **, $P < 0.01$; ***, $P < 0.001$). ns, nonsignificant. C, signaling molecules were analyzed by Western blotting in LK cells from splenocytes of CT26 TBM. D, incorporated BrdUrd in LK cells was measured in the *in vitro* cultured total splenocytes from CT26 TBM with or without 20 μmol/L PD98059 and 2 μg/mL rmOpn. The data are representative of three independent experiments and represent the mean ± SEM (*, $P < 0.05$; **, $P < 0.01$; ***, $P < 0.001$).

of CT26shOpn-injected mice than they were in the CT26pGIPZ-injected group. These results strongly suggest that the increased expression of CD44 and/or CD49d in splenic LK cells in TBM might be responsible for the proliferation of this cell population in this experimental setting. To further clarify which receptor mediates the observed osteopontin-induced LK cell proliferation, we employed blocking antibodies against CD44, CD49d, or CD51. Interestingly, anti-CD44 almost completely abolished the BrdUrd uptake of LK cells in response to osteopontin (Fig. 5B). Anti-CD49d also slightly inhibited BrdUrd uptake by LK cells to a lesser extent. Collectively, these results indicate that the upregulation of CD44 on splenic LK cells triggered the osteopontin-mediated proliferation of this cell population in TBM.

Tumor-derived osteopontin triggered Erk1/2-MAPK signal transduction in LK cells

To further determine the molecular mechanism by which osteopontin induces LK cell expansion, we investigated the intracellular signal transduction triggered by osteopontin. Splenic LK cells were isolated from CT26 TBM and stimulated with osteopontin. As shown in Fig. 5C, the levels of phospho-Erk1/2, cyclinD1, and phospho$^{(Ser807/811)}$-Rb were increased by osteopontin and were almost completely reversed by the Erk1/2-specific inhibitor PD98059. Consistent with this notion, the addition of PD98059 completely suppressed the osteopontin-induced expansion of the LK population *in vitro* (Fig. 5D). Moreover, the increased level of pERK induced by osteopontin was reversed by pretreatment with an anti-CD44 antibody (Supplementary Fig. S9). Thus, osteopontin induced the expansion of LK cells by activating Erk1/2-MAPK signaling transduction and, consequently, the phosphorylation of Rb through the cyclinD1/CDK complex.

Antiosteopontin enhances antitumor therapeutic effect of cell-based immunotherapeutic vaccine

Our findings demonstrate a detrimental role for tumor-derived osteopontin. Thus, we determined whether the blockade

Published OnlineFirst October 1, 2014; DOI: 10.1158/0008-5472.CAN-14-1482

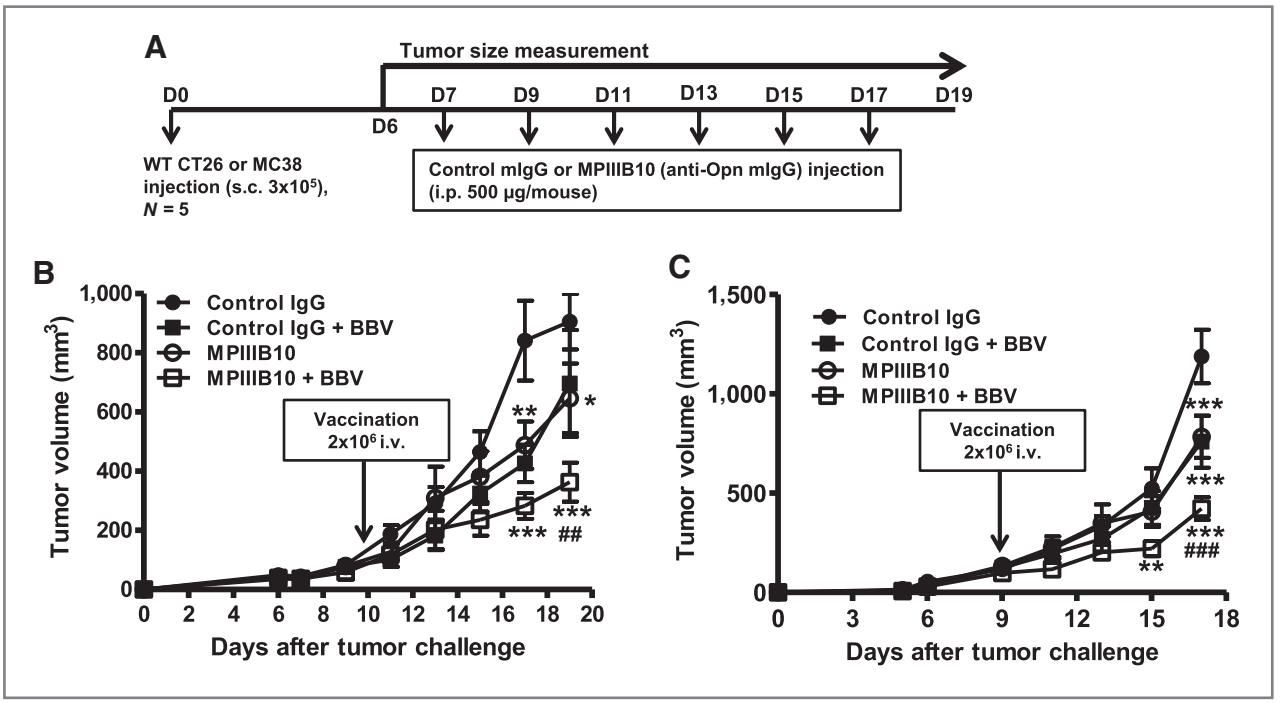

Figure 6. Antiosteopontin enhanced the antitumor therapeutic effect of a B-cell–based immunotherapeutic vaccine. A, Balb/c mice or C57BL/6 mice were subcutaneously injected with 3×10^5 CT26 or MC38 cells, respectively. Seven days after tumor injection, 0.5 mg of IgG (control) or MPIIIB10 (anti-Opn mIgG) was injected intraperitoneally into mice and tumor size was measured ($n = 5$). B, tumor volume of the CT26 implanted Balb/c mice tumor model. The B-cell–based immunotherapeutic vaccine was used as an additional treatment at day 10. The data are representative of two independent experiments and represent the mean ± SEM. C, tumor volume of MC38 implanted C57BL/6 mice tumor model. Some animals were also treated with B-cell–based immunotherapeutic vaccines at day 9. The data represent the mean ± SEM, and a two-way ANOVA analysis was used to determine differences between multiple groups (*, $P < 0.05$; **, $P < 0.01$; ***, $P < 0.001$, compared with control IgG group, #, $P < 0.05$; ##, $P < 0.01$, compared with control IgG and BBV group)

of osteopontin activity enhances antitumor immunity alone or in combination with tumor-vaccine approaches. To this end, we employed a B-cell–based antitumor vaccine (31, 32). We have convincingly showed that a NKT ligand-loaded, B-cell–based vaccine elicits tumor-specific immune responses (21, 33, 34). We subcutaneously inoculated Balb/c mice with CT26 tumor cells on day 0 and then intraperitoneally injected the mice with 0.5 mg of antiosteopontin (MPIIIB10) or mIgG as a control every other day for 10 days (Fig. 6A). Some mice were also given a B-cell–based vaccine on day 10. As expected, mice receiving the B-cell–based vaccine showed delayed tumor growth. Notably, we also observed that tumor growth was moderately but significantly inhibited in antiosteopontin-treated mice compared with control IgG-treated mice. Furthermore, antiosteopontin significantly delayed tumor growth in mice treated with the B-cell–based vaccine (Fig. 6B). A similar inhibition of tumor growth by antiosteopontin alone and in combination with a B-cell–based vaccine was observed when the MC38 tumor model was used instead (Fig. 6C). These results demonstrate that the blockade of osteopontin activity not only suppresses tumor growth but also enhances the antitumor immunity induced by an antitumor vaccine.

Discussion

In this study, we investigated the role of tumor-derived osteopontin on tumor progression and antitumor immunity. Using two different tumor models in animals, we found that (i) tumor-derived osteopontin increased the levels of osteopontin in the circulation; (ii) tumor-derived osteopontin was responsible for the increased LK cell population and the subsequent accumulation of MDSCs in the spleen of tumor-bearing hosts in a CD44-dependent manner via the Erk1/2–MAPK–Rb signaling pathway; and (iii) the blockade of osteopontin suppressed tumor growth and significantly enhanced the antitumor immunity induced by a cellular tumor vaccine. Hence, our findings unveil a novel mechanism by which tumor cells induce a protumorigenic microenvironment by mediating extramedullary hematopoiesis. Moreover, our results provide a fundamental basis for the use of osteopontin inhibitors in cancer treatment and in improving the efficacy of anticancer therapeutic vaccines.

Recent studies have suggested that the spleen emerged as a myeloid reservoir and is responsible for generating immunosuppressive myeloid cells in inflammatory conditions (20, 35, 36). Consistently, we observed an increase in LSK and LK cells in the spleen (Fig. 1A and 1B), and these increased progenitor cells were dominantly converted into MDSCs in TBM (Fig. 1C and D and Supplementary Fig. S2E). Although various tumor-derived factors and inflammatory mediators should be involved in extramedullary myelopoiesis, specific critical factors remain unidentified. In this study, we found that osteopontin was augmented in CT26

Published OnlineFirst October 1, 2014; DOI: 10.1158/0008-5472.CAN-14-1482

and MC38 TBM, which was mainly derived from tumors (Fig. 2 and Supplementary Fig. S4A and S4B). Because tumors express 160-fold more osteopontin mRNA than does Mo MDSC, the entire increase of osteopontin in TBM might be exclusively derived from tumor cells rather than Mo MDSCs (Fig. 2D and E).

Osteopontin is abundantly found in the extracellular matrix and body fluids (37–39) and is primarily known as bone sialoprotein (40). Recently, several reports have shown that the overexpression of osteopontin in various tumors is profoundly related to the growth and metastasis of several solid tumors (41–43) and have suggested the use of osteopontin as a prognosis marker for the prediction of tumor malignancy (23, 44–46). Consistent with these previous results, we observed that the lentiviral knockdown of osteopontin significantly inhibited *in vivo* tumor growth (Figs. 3D and 4B) without affecting the *in vitro* proliferation of CT26 cells (Fig. 3B and C), suggesting that osteopontin is crucial for establishing the tumorigenic environment by supporting tumor growth *in vivo*. Consistent with this concept, osteopontin has been shown to mediate angiogenesis (47) by inducing IL1β production from monocytes that can mediate the chemotaxis of endothelial cells (48). In addition to the inhibition of tumor growth, we focused on the novel roles of osteopontin in tumor-derived extramedullary myelopoiesis. Mice bearing CT26shOpn showed a reduced expansion of splenic LK cells, but the expansion of LSK cells (precursor of LK cells) was not significantly affected (Fig. 3F). This result suggests that tumor-derived osteopontin affects the expansion of peripheral LK cells and subsequently contributes to the accumulation of MDSCs in the tumor context.

Recently, MDSCs have been suggested to be precursors of osteoclasts under tumor environment (49, 50). Considering that osteopontin is a main component of the bone microenvironment (39), osteopontin might induce the proliferation of LK cells and subsequently expand the MDSCs that may serve as precursors of osteoclasts in the bone. As osteopontin enhances the migration of neutrophils (51), it is possible to surmise that tumor-derived osteopontin promotes the migration of neutrophilic PMN MDSCs to the tumor site. Further investigation is needed to determine the role of osteopontin during the differentiation of MDSCs to osteoclasts as well as its role in the migration of PMN MDSC in tumor-bearing hosts.

The role of osteopontin in the proliferation of stem cells or progenitor cells remains controversial. For instance, several reports have shown that osteopontin is a key component of the hematopoietic stem cell niche and negatively regulates hematopoietic stem cells in the bone marrow (29, 30). In this study, osteopontin induced the proliferation of splenic LK cells in TBM, whereas bone marrow LK cells were comparable with naïve mice (Fig. 4C). As the physiologic environment is quite different between the spleen and bone marrow, the role of osteopontin might depend on the surrounding environment of LK cells. This result was further supported by results showing recombinant osteopontin-induced splenic LK cell expansion in the naïve mice (Fig. 4E), which indicates that osteopontin is directly associated with the expansion of LK cells.

Osteopontin-triggered signal transduction via integrins or CD44 is primarily related to the evasion, migration, and proliferation of tumor cells (26, 41). We observed upregulated CD44 on LK cells in TBM, which then triggered the osteopontin-mediated proliferation of this cell population (Fig. 5A and B). Furthermore, we observed that osteopontin triggered the Erk1/2–MAPK signaling cascade and consequently phosphorylated Rb (Fig. 5C), which could induce the proliferation of LK cells (Fig. 5D). Because of the redundancies and complexities in signal transduction, it is difficult to determine the contribution of each of the osteopontin receptors and respective downstream signaling events on the osteopontin-mediated proliferation of LK cells. Although the ERK1/2–MAPK pathway is one of the downstream signal transduction cascades triggered by CD44 (Supplementary Fig. S9), further studies should be conducted to uncover the precise relation between osteopontin-CD44 ligation and CD44-mediated ERK1/2–MAPK signaling and its quantitative contribution on osteopontin-mediated LK cell proliferation. In addition, because of the rare frequency of the LK cell population in the spleen, further description of the osteopontin-related specific subpopulations of these cells is limited. Therefore, specific myeloid progenitors that expand in the presence of osteopontin would be defined in future studies.

Blocking abnormal myelopoiesis would fundamentally eliminate the tumor-derived immunosuppressive environment though the prevention of MDSC generation and the subsequent establishment of a tumor-derived immunosuppressive network (5). In this regard, we targeted osteopontin in TBM and this strategy moderately but significantly delayed tumor growth, despite osteopontin acting as one of several factors that mediate tumor-derived extramedullary myelopoiesis. Furthermore, the blockade of osteopontin activity not only suppressed tumor growth but also significantly synergized with B-cell–based immunotherapeutic vaccines in mediating antitumor immunity (Fig. 6). Both breaking the tumor-derived immunosuppressive environment and inducing strong immune responses against tumor antigens are necessary to eliminate established tumors. In this regard, a combination of osteopontin blockade and general anticancer vaccine strategies could be useful for improving the efficacy of anticancer vaccines by alleviating the tumor-derived immunosuppressive environment.

In this study, we unveiled novel roles of tumor-derived osteopontin in extramedullary myelopoiesis. Tumor-derived osteopontin aggravates the immunosuppressive environment by enhancing extramedullary myelopoiesis and the subsequent accumulation of MDSCs. Furthermore, the blockade of osteopontin improved the anticancer activity of a cell-based immunotherapeutic vaccine. Our findings provide a fundamental basis for the use of osteopontin inhibitors in cancer treatment and in improving the efficacy of anticancer therapeutic vaccines, collectively suggesting osteopontin as a potential therapeutic target.

Published OnlineFirst October 1, 2014; DOI: 10.1158/0008-5472.CAN-14-1482

Disclosure of Potential Conflicts of Interest

No potential conflicts of interest were disclosed.

Authors' Contributions

Conception and design: E.-K. Kim, K.-A. Lee, C.-Y. Kang
Development of methodology: E.-K. Kim
Acquisition of data (provided animals, acquired and managed patients, provided facilities, etc.): E.-K. Kim, Y. Jang
Analysis and interpretation of data (e.g., statistical analysis, biostatistics, computational analysis): E.-K. Kim, B. Song
Writing, review, and/or revision of the manuscript: E.-K. Kim, Y.-J. Park, Y. Chung, C.-Y. Kang
Administrative, technical, or material support (i.e., reporting or organizing data, constructing databases): E.-K. Kim, I. Jeon, H. Seo, C.-Y. Kang
Study supervision: C.-Y. Kang

Acknowledgments

This work was supported by Public Welfare and Safety Research program (20110020963) through the National Research Foundation of Korea (NRF) funded by the Ministry of Science, ICT and Future Planning, National R& D Program for Cancer Control (0720500) funded by the Ministry of Health and Welfare and BK21 Plus Program (10220130000017) of the National Research Foundation of Korea funded by the Ministry of Education.

The costs of publication of this article were defrayed in part by the payment of page charges. This article must therefore be hereby marked *advertisement* in accordance with 18 U.S.C. Section 1734 solely to indicate this fact.

Received May 19, 2014; revised August 16, 2014; accepted September 1, 2014; published OnlineFirst October 1, 2014.

References

1. Sica A, Porta C, Morlacchi S, Banfi S, Strauss L, Rimoldi M, et al. Origin and functions of tumor-associated myeloid cells (TAMCs). Cancer Microenviron 2011;5:133–49.
2. Galdiero MR, Bonavita E, Barajon I, Garlanda C, Mantovani A, Jaillon S. Tumor associated macrophages and neutrophils in cancer. Immunobiology 2013;218:1402–10.
3. Murdoch C, Muthana M, Coffelt SB, Lewis CE. The role of myeloid cells in the promotion of tumour angiogenesis. Nat Rev Cancer 2008;8:618–31.
4. Youn JI, Nagaraj S, Collazo M, Gabrilovich DI. Subsets of myeloid-derived suppressor cells in tumor-bearing mice. J Immunol 2008;181:5791–802.
5. Lindau D, Gielen P, Kroesen M, Wesseling P, Adema GJ. The immunosuppressive tumour network: myeloid-derived suppressor cells, regulatory T cells and natural killer T cells. Immunology 2013;138:105–15.
6. Liu C, Yu S, Kappes J, Wang J, Grizzle WE, Zinn KR, et al. Expansion of spleen myeloid suppressor cells represses NK cell cytotoxicity in tumor-bearing host. Blood 2007;109:4336–42.
7. Bronte V. Myeloid-derived suppressor cells in inflammation: uncovering cell subsets with enhanced immunosuppressive functions. Eur J Immunol 2009;39:2670–2.
8. Corzo CA, Cotter MJ, Cheng P, Cheng F, Kusmartsev S, Sotomayor E, et al. Mechanism regulating reactive oxygen species in tumor-induced myeloid-derived suppressor cells. J Immunol 2009;182:5693–701.
9. Ostrand-Rosenberg S, Sinha P. Myeloid-derived suppressor cells: linking inflammation and cancer. J Immunol 2009;182:4499–506.
10. Rodriguez PC, Ernstoff MS, Hernandez C, Atkins M, Zabaleta J, Sierra R, et al. Arginase I-producing myeloid-derived suppressor cells in renal cell carcinoma are a subpopulation of activated granulocytes. Cancer Res 2009;69:1553–60.
11. Nagaraj S, Schrum AG, Cho HI, Celis E, Gabrilovich DI. Mechanism of T cell tolerance induced by myeloid-derived suppressor cells. J Immunol 2010;184:3106–16.
12. Ostrand-Rosenberg S. Myeloid-derived suppressor cells: more mechanisms for inhibiting antitumor immunity. Cancer Immunol Immunother 2010;59:1593–600.
13. Lechner MG, Megiel C, Russell SM, Bingham B, Arger N, Woo T, et al. Functional characterization of human Cd33+ and Cd11b+ myeloid-derived suppressor cell subsets induced from peripheral blood mononuclear cells co-cultured with a diverse set of human tumor cell lines. J Transl Med 2011;9:90.
14. Obermajer N, Muthuswamy R, Odunsi K, Edwards RP, Kalinski P. PGE2-Induced CXCL12 production and CXCR4 expression controls the accumulation of human MDSCs in ovarian cancer environment. Cancer Res 2011;71:7463–70.
15. Youn JI, Kumar V, Collazo M, Nefedova Y, Condamine T, Cheng P, et al. Epigenetic silencing of retinoblastoma gene regulates pathologic differentiation of myeloid cells in cancer. Nat Immunol 2013;14:211–20.
16. Sevko A, Umansky V. Myeloid-derived suppressor cells interact with tumors in terms of myelopoiesis, tumorigenesis and immunosuppression: thick as thieves. J Cancer 2013;4:3–11.
17. Balducci L, Hardy C. High proliferation of granulocyte-macrophage progenitors in tumor-bearing mice. Cancer Res 1983;43:4643–7.
18. O'Malley DP. Benign extramedullary myeloid proliferations. Modern Pathology 2007;20:405–15.
19. Swirski FK, Nahrendorf M, Etzrodt M, Wildgruber M, Cortez-Retamozo V, Panizzi P, et al. Identification of splenic reservoir monocytes and their deployment to inflammatory sites. Science 2009;325:612–6.
20. Cortez-Retamozo V, Etzrodt M, Newton A, Rauch PJ, Chudnovskiy A, Berger C, et al.Origins of tumor-associated macrophages and neutrophils. Proc Natl Acad Sci U S A 2012;109:2491–6.
21. Kim EK, Seo HS, Chae MJ, Jeon IS, Song BY, Park YJ, et al. Enhanced antitumor immunotherapeutic effect of B-cell-based vaccine transduced with modified adenoviral vector containing type 35 fiber structures. Gene Ther 2014;21:106–14.
22. Yang JC, Perry-Lalley D. The envelope protein of an endogenous murine retrovirus is a tumor-associated T-cell antigen for multiple murine tumors. J Immunother 2000;23:177–83.
23. Agrawal D, Chen T, Irby R, Quackenbush J, Chambers AF, Szabo M, et al. Osteopontin identified as colon cancer tumor progression marker. C R Biol 2003;326:1041–3.
24. Behera R, Kumar V, Lohite K, Karnik S, Kundu GC. Activation of JAK2/STAT3 signaling by osteopontin promotes tumor growth in human breast cancer cells. Carcinogenesis 2009;31:192–200.
25. Chakraborty G, Jain S, Kundu GC. Osteopontin promotes vascular endothelial growth factor-dependent breast tumor growth and angiogenesis via autocrine and paracrine mechanisms. Cancer Res 2008;68:152–61.
26. Luo X, Ruhland MK, Pazolli E, Lind AC, Stewart SA. Osteopontin stimulates preneoplastic cellular proliferation through activation of the MAPK pathway. Mol Cancer Res 2011;9:1018–29.
27. McAllister SS, Gifford AM, Greiner AL, Kelleher SP, Saelzler MP, Ince TA, et al. Systemic endocrine instigation of indolent tumor growth requires osteopontin. Cell 2008;133:994–1005.
28. Mi Z, Bhattacharya SD, Kim VM, Guo H, Talbot LJ, Kuo PC. Osteopontin promotes CCL5-mesenchymal stromal cell-mediated breast cancer metastasis. Carcinogenesis 2011;32:477–87.
29. Nilsson SK, Johnston HM, Whitty GA, Williams B, Webb RJ, Denhardt DT, et al. Osteopontin, a key component of the hematopoietic stem cell niche and regulator of primitive hematopoietic progenitor cells. Blood 2005;106:1232–9.
30. Grassinger J, Haylock DN, Storan MJ, Haines GO, Williams B, Whitty GA, et al. Thrombin-cleaved osteopontin regulates hemopoietic stem and progenitor cell functions through interactions with 9 1 and 41 integrins. Blood 2009;114:49–59.
31. Chung Y, Kim BS, Kim YJ, Ko HJ, Ko SY, Kim DH, et al. CD1d-restricted T cells license B cells to generate long-lasting cytotoxic antitumor immunity *in vivo*. Cancer Res 2006;66:6843–50.

Published OnlineFirst October 1, 2014; DOI: 10.1158/0008-5472.CAN-14-1482

32. Kim YJ, Han SH, Kang HW, Lee JM, Kim YS, Seo JH, et al. NKT ligand-loaded, antigen-expressing B cells function as long-lasting antigen presenting cells *in vivo*. Cell Immunol 2011;270:135–44.
33. Kim YS, Kim YJ, Lee JM, Han SH, Ko HJ, Park HJ, et al. CD40-targeted recombinant adenovirus significantly enhances the efficacy of antitumor vaccines based on dendritic cells and B cells. Hum Gene Ther 2010;21:1697–706.
34. Kim YJ, Ko HJ, Kim YS, Kim DH, Kang S, Kim JM, et al. alpha-Galactosylceramide-loaded, antigen-expressing B cells prime a wide spectrum of antitumor immunity. Int J Cancer 2008;122:2774–83.
35. Swirski FK, Nahrendorf M, Etzrodt M, Wildgruber M, Cortez-Retamozo V, Panizzi P, et al. Identification of splenic reservoir monocytes and their deployment to inflammatory sites. Science 2009;325:612–6.
36. Cortez-Retamozo V, Etzrodt M, Newton A, Ryan R, Pucci F, Sio SW, et al. Angiotensin II drives the production of tumor-promoting macrophages. Immunity 2013;38:296–308.
37. Wang KX, Denhardt DT. Osteopontin: role in immune regulation and stress responses. Cytokine Growth Factor Rev 2008;19:333–45.
38. Bellahcene A, Castronovo V, Ogbureke KU, Fisher LW, Fedarko NS. Small integrin-binding ligand N-linked glycoproteins (SIBLINGs): multifunctional proteins in cancer. Nat Rev Cancer 2008;8:212–26.
39. Denhardt DT, Noda M. Osteopontin expression and function: role in bone remodeling. J Cell Biochem Suppl 1998;30–31:92–102.
40. Reinholt FP, Hultenby K, Oldberg A, Heinegard D. Osteopontin–a possible anchor of osteoclasts to bone. Proc Natl Acad Sci U S A 1990;87:4473–5.
41. Rangaswami H, Bulbule A, Kundu GC. Osteopontin: role in cell signaling and cancer progression. Trends Cell Biol 2006;16:79–87.
42. Zhou Y, Dai DL, Martinka M, Su M, Zhang Y, Campos EI, et al. Osteopontin expression correlates with melanoma invasion. J Invest Dermatol 2005;124:1044–52.
43. Wai PY. Osteopontin silencing by small interfering RNA suppresses in vitro and in vivo CT26 murine colon adenocarcinoma metastasis. Carcinogenesis 2005;26:741–51.
44. Liersch R, Gerss J, Schliemann C, Bayer M, Schwoppe C, Biermann C, et al. Osteopontin is a prognostic factor for survival of acute myeloid leukemia patients. Blood 2012;119:5215–20.
45. Said HM, Katzer A, Flentje M, Vordermark D. Response of the plasma hypoxia marker osteopontin to in vitro hypoxia in human tumor cells. Radiother Oncol 2005;76:200–5.
46. Chen RX, Xia YH, Cui JF, Xue TC, Ye SL. Osteopontin, a single marker for predicting the prognosis of patients with tumor-node-metastasis stage I hepatocellular carcinoma after surgical resection. J Gastroenterol Hepatol 2010;25:1435–42.
47. Bandopadhyay M, Bulbule A, Butti R, Chakraborty G, Ghorpade P, Ghosh P, et al. Osteopontin as a therapeutic target for cancer. Expert Opin Ther Targets 2014;18:883–95.
48. Naldini A, Leali D, Pucci A, Morena E, Carraro F, Nico B, et al. Cutting edge: IL-1beta mediates the proangiogenic activity of osteopontin-activated human monocytes. J Immunol 2006;177:4267–70.
49. Sawant A, Ponnazhagan S. Myeloid-derived suppressor cells as osteoclast progenitors: a novel target for controlling osteolytic bone metastasis. Cancer Res 2013;73:4606–10.
50. Zhuang J, Zhang J, Lwin ST, Edwards JR, Edwards CM, Mundy GR, et al. Osteoclasts in multiple myeloma are derived from Gr-1+CD11b+myeloid-derived suppressor cells. PLoS ONE 2012;7:e48871.
51. Koh A, da Silva APB, Bansal AK, Bansal M, Sun C, Lee H, et al. Role of osteopontin in neutrophil function. Immunology 2007;122:466–75.

Published OnlineFirst October 1, 2014; DOI: 10.1158/0008-5472.CAN-14-1482

Cancer Research

Tumor-Derived Osteopontin Suppresses Antitumor Immunity by Promoting Extramedullary Myelopoiesis

Eun-Kyung Kim, Insu Jeon, Hyungseok Seo, et al.

Cancer Res Published OnlineFirst October 1, 2014.